for metal-metal bonding will be those not involved in metal-ligand σ-bonding (d_{xz}, d_{yz}, d_{xy} orbitals on the metal atom). From the analyses of McCarley et al.,[36] Hoffmann et al.,[37] Wentworth et al.,[38] and Cotton et al.[39] there are three bonding molecular orbitals in D_{3h} symmetry ($a_1' < e' < e'' < a_2''$), where the $\sigma(a_1')$ and $\pi(e')$ orbitals are bonding and the $\pi(e'')$ and $\pi(a_2'')$ orbitals are antibonding. The descent in symmetry to C_{2v} converts them to the following representations: $a'(\sigma) \rightarrow a_1$, $a_2''(\sigma^*) \rightarrow b_2$, $e'(\pi_1) \rightarrow a_1$, $e'(\pi_2) \rightarrow b_1$, $e''(\pi_3^*) \rightarrow b_2$, and $e''(\pi_4^*) \rightarrow a_2$. The a_1 MO remains a σ bond of the lowest energy of the set, which is occupied with two electrons, whereas the $a_1(\pi)$ and $b_1(\pi)$ orbitals are occupied by the remaining four electrons. Thus the formal metal-metal bond order in **2** is 3 ($\sigma^2\pi^4$). Note, the two π orbitals are not degenerate in C_{2v}. Again from McCarley's argumentation, the b_1 π orbital may be lower in energy than the $a_1\pi$ orbital and the ground state in **2** may be described as $[\sigma(a_1)]^2[\pi(b_1)]^2[\pi(a_1)]^2$ and the observed two low-energy transitions in the electronic spectrum of (**2**) (Figure 1) may be assigned to allowed $\pi(a_1) \rightarrow \pi^*(a_1)$ and $\pi(a_1) \rightarrow \pi^*(b_1)$. In **3** the ground state then is $[\sigma(a_1)]^2[\pi(b_1)]^2[\pi(a_1)]^1$; one electron of **2** is removed from a bonding metal-metal MO, and consequently, the Mo-Mo bond in **3** is longer than that in **2** and the bond order is 2.5. The electrochemically generated mixed-valence $Mo^{II}Mo^{III}$ species would have to accommodate the additional electron in an antibonding metal-metal $\pi^*(a_1)$ orbital, and also an increase of the Mo-Mo bond is expected (the bond order is again 2.5).

Conclusion

We have shown in this study that the classical Werner-type complex **1** is reversibly transformed by deprotonation at the bridging hydroxo group into a metal-metal-bonded (μ-oxo)bis(μ-acetato)dimolybdenum(III) species (bond order 3). This intramolecular base-induced Mo-Mo bond formation is unprecedented and is believed to be a consequence of the substantial Mo-O bond contraction on going from a μ-hydroxo to an μ-oxo bridge, which brings the Mo(III) centers in close enough proximity to induce an overlap of the metal d_{xy}, d_{xz}, d_{yz} orbitals to form a weak Mo-Mo triple bond ($\sigma^2\pi^4$). This observation is nicely corroborated by the ease of a one-electron oxidation of **2** to produce **3** with a slightly longer Mo-Mo bond of order 2.5 ($\sigma^2\pi^3$).

Acknowledgment. We thank the Fonds der Chemischen Industrie for financial support of this work. A.N. is grateful to CNPq (Brazil) for a stipend during 1987. We thank Prof. W. Haase and Dipl.-Ing. S. Gehring (Universität Darmstadt) for measurements of temperature-dependent magnetic susceptibilities.

Registry No. **1**$(PF_6)_3$, 114198-91-3; **1**$(ClO_4)_3 \cdot H_2O$, 114198-93-5; **2**$(PF_6)_2 \cdot 3H_2O$, 118335-23-2; **2**$(ClO_4)(BF_4) \cdot H_2O$, 114198-97-9; **3**$(PF_6)_3$, 118335-25-4; **3**$(ClO_4)_3 \cdot H_2O$, 118335-27-6; $LMoBr_3$, 94370-80-6; $[L_2Mo^{II}Mo^{III}(\mu\text{-}O)(\mu\text{-}CH_3CO_2)_2]^+$, 118335-28-7; Mo, 7439-98-7.

Supplementary Material Available: Tables listing bond lengths (Tables SI-SIII), bond angles (Tables SIV-SVI), derived hydrogen positions (Tables SVII-SIX), and anisotropic temperature factors (Tables SX-SXII) and a full table of crystal data (Table SXIII) for structures **1-3**, respectively (14 pages); tables of calculated and observed structure factors (94 pages). Ordering information is given on any current masthead page.

(36) Templeton, J. L.; Dorman, W. C.; Clardy, J. C.; McCarley, R. E. *Inorg. Chem.* **1978**, *17*, 1263.
(37) Summerville, R. H.; Hoffmann, R. *J. Am. Chem. Soc.* **1979**, *101*, 3821.
(38) Saillant, R.; Wentworth, R. A. D. *J. Am. Chem. Soc.* **1969**, *91*, 2174.
(39) (a) Cotton, F. A.; Ucko, D. A. *Inorg. Chim. Acta* **1972**, *6*, 161. (b) Cotton, F. A. *Pure Appl. Chem.* **1967**, *17*, 25.
(40) Cotton, F. A.; Diebold, M. P.; O'Connor, C. J.; Powell, G. L. *J. Am. Chem. Soc.* **1985**, *107*, 7438.

Contribution from the Department of Chemistry, Colorado State University, Fort Collins, Colorado 80523

Five- and Six-Coordinate High-Spin Iron(III) Porphyrin Complexes with Teflate ($OTeF_5^-$) Ligands

Patti J. Kellett,[‡] Michael J. Pawlik, Lucille F. Taylor, Ronald G. Thompson, Mark A. Levstik, Oren P. Anderson, and Steven H. Strauss*,[1]

Received June 14, 1988

The compounds Fe(TPP)($OTeF_5$) and Fe(OEP)($OTeF_5$), together with their ^{18}O analogues, were prepared and characterized by using magnetic susceptibility measurements and ^1H and ^{19}F NMR, UV-vis, and mid- and far-infrared spectroscopy. The solution behavior of Fe(TPP)($OTeF_5$) was investigated by cyclic voltammetry and ligand replacement reactions. The data indicate that these complexes contain high-spin iron(III) and that the relative ligand field strength of the $OTeF_5^-$ anion follows the order $Cl^- > OTeF_5^- > ClO_4^-$. The compound Fe(TPP)($OTeF_5$)(THF) was examined by single-crystal X-ray diffraction. This compound crystallized in the triclinic system, space group $P\bar{1}$ ($Z = 1$), with $a = 9.524$ (3) Å, $b = 11.069$ (2) Å, $c = 11.843$ (3) Å, $\alpha = 102.64$ (2)°, $\beta = 104.45$ (2)°, and $\gamma = 114.44$ (2)°. The $OTeF_5^-$ and THF ligands were disordered; the best model placed the $OTeF_5^-$ ligand above the porphyrin plane 65% of the time. The Fe-N_p distances of 2.064 (5), 2.011 (5), 2.047 (5), and 2.086 (4) Å are indicative of high-spin ($S = {}^5/_2$) iron(III). The iron atom is displaced toward the $OTeF_5^-$ ligand by 0.20 Å, the Fe-O($OTeF_5$) distance is 1.967 (5) Å, and Fe-O(THF) is 2.334 (7) Å. This is only the second structurally characterized six-coordinate high-spin iron(III) porphyrin complex with different axial ligands.

Introduction

Despite the well-developed use of pentafluoroorthotellurate ($OTeF_5$) as a bulky and electronegative substituent for main-group elements (e.g. $Xe(OTeF_5)_2$,[2] $B(OTeF_5)_3$,[3] $I(OTeF_5)_5$[4]),[5] the chemistry of $OTeF_5^-$ (teflate) as a ligand for transition metals, especially in oxidation states ≤ 3, has only recently been explored.[6,7] One of our goals is to make use of any unique electronic, steric, and structural properties of teflate to modify the chemical properties of metal ions in new ways. If this is to be done in a rational way, the properties of teflate as a ligand must be fully

[‡] Formerly Patti K. Miller.

(1) Alfred P. Sloan Fellow, 1987-1989.
(2) Sladky, F. *Monatsh. Chem.* **1970**, *101*, 1559.
(3) (a) Kropshofer, H.; Leitzke, O.; Peringer, P.; Sladky, F. *Chem. Ber.* **1981**, *114*, 2644. (b) Sawyer, J. F.; Schrobilgen, G. J. *Acta Crystallogr., Sect. B: Struct. Crystallogr. Cryst. Chem.* **1982**, *B38*, 1561.
(4) Seppelt, K.; Lentz, D. *Z. Anorg. Allg. Chem.* **1980**, *460*, 5.
(5) (a) Seppelt, K. *Angew. Chem., Int. Ed. Engl.* **1982**, *21*, 877. (b) Engelbrecht, A.; Sladky, F. *Adv. Inorg. Chem. Radiochem.* **1981**, *24*, 189. (c) Seppelt, K. *Acc. Chem. Res.* **1979**, *12*, 211.

0020-1669/89/1328-0440$01.50/0

understood. To this end, metal teflate complexes that have well-studied analogues with halide, alkoxide, perchlorate, and triflate ligands are being prepared and characterized in our laboratory.

Our interest in and experience with iron porphyrins (Por[8]) and related compounds made the preparation of Fe(Por)($OTeF_5$) complexes a logical goal.[9] Due in large part to their importance as models for active sites in heme proteins and enzymes, Fe(Por)(X) complexes[8] have been studied by a full complement of physicochemical techniques and are among the best characterized transition-metal complexes.[10] In this paper we report the synthesis, characterization, and solution behavior of Fe(OEP)($OTeF_5$) and Fe(TPP)($OTeF_5$) and their ^{18}O equivalents.[8] We also report the structure of Fe(TPP)($OTeF_5$)(THF), which crystallized from a tetrahydrofuran (THF) solution of Fe(TPP)($OTeF_5$). This complex is only the second example of an iron(III) porphyrin that is high-spin ($S = {}^5/_2$) and has two different axial ligands.

Experimental Section

General Procedures. In the following preparations and physical measurements, all operations were carried out with rigorous exclusion of dioxygen and water.[11] Schlenk, glovebox, and high-vacuum techniques were employed, with purified dinitrogen used when an inert atmosphere was required.

Reagents and Solvents. The following solvents were dried by distillation from the indicated drying agent: tetrahydrofuran (Na), toluene (Na), dichloromethane (P_2O_5), dichloromethane-d_2 (4-Å sieves), chloroform-d (4-Å sieves), hexane (Na), ethyl acetate (CaH_2). Heptane was used as received. The compounds $HOTeF_5$,[12] $H^{18}OTeF_5$,[13] $[AgOTeF_5(CH_3CN)_2]_2$,[6b] $[N(n\text{-}Bu)_4^+][OTeF_5^-]$,[12] $[Fe(TPP)]_2O$,[9f] $[Fe(OEP)]_2O$,[9f] and Fe(TPP)(ClO_4)[14] were prepared by published procedures. Water was removed from an ethyl acetate solution of $N(n\text{-}Bu)_4^+Cl^-$ (Aldrich) by azeotropic distillation. The anhydrous crystalline salt was dried under vacuum at room temperature to remove any traces of ethyl acetate.

Physical Methods. Samples for ^1H NMR spectroscopy were dichloromethane-d_2 or chloroform-d solutions sealed under vacuum in 5-mm NMR tubes. The concentrations varied from 5 to 10 mM. Spectra were recorded on a Bruker WP200SY spectrometer operating at 200.13 MHz. Chemical shifts (δ scale) are relative to Me_4Si. The probe temperature was monitored by the method of Van Geet.[15] Samples for ^{19}F NMR spectroscopy were dichloromethane-d_2 or chloroform-d solutions sealed under vacuum in 5-mm NMR tubes. The concentrations were ~10 mM. Spectra were recorded on a Bruker WP200SY spectrometer operating at 188.31 MHz. Chemical shifts are relative to $CFCl_3$. Samples for IR spectroscopy were Nujol mulls (between KBr windows for mid-IR spectra or polyethylene windows for far-Ir spectra) or dichloromethane or tetrahydrofuran solutions (0.2 mm path length KBr cells). Spectra were recorded on a Perkin-Elmer 983 or Nicolet 60SX spectrometer calibrated with polystyrene. Band positions are ±1 cm^{-1}. Samples for UV–vis spectroscopy were dichloromethane, toluene, or tetrahydrofuran solutions. Spectra were recorded on a Perkin-Elmer λ3B spectrophotometer.

A Bioanalytical Systems BAS-100 electrochemical analyzer was used for all electrochemical measurements, which were made with a platinum-disk electrode, freshly dried and distilled dichloromethane, and 0.10 M $[N(n\text{-}Bu)_4^+][ClO_4^-]$ or $[N(n\text{-}Bu)_4^+][OTeF_5^-]$ as supporting electrolyte. The concentration of the metal complex was kept between 1 and 2 mM. $E_{1/2}$ values were measured by cyclic voltammetry using a conventional three-electrode configuration with a saturated calomel reference electrode separated from the bulk of the solution by a fritted-glass disk and a Luggin capillary.

Solid-state magnetic susceptibilities (duplicate samples) were measured at room temperature by the Faraday method with the use of a Cahn-Ventron 7600 magnetic susceptibility system with a Model RTL minibalance. The compound $HgCo(SCN)_4$ was used as the susceptibility calibrant. Finely ground, recrystallized (dichloromethane/heptane), vacuum-dried samples of Fe(TPP)($OTeF_5$) and Fe(OEP)($OTeF_5$) were used. Diamagnetic corrections were taken from the literature for TPP,[16] OEP,[9b] Fe,[17] O,[17] Te,[17] and F.[17] Susceptibility measurements were not made for solid samples of Fe(TPP)($OTeF_5$)(THF), since crystals of this compound readily lose the coordinated THF ligand.

Preparation of Compounds. Fe(TPP)($OTeF_5$) and Fe(TPP)($^{18}OTeF_5$). A toluene solution (20 mL) of $[Fe(TPP)]_2O$ (150 mg, 0.11 mmol) was treated with a 14% excess of $HOTeF_5$ (60 mg, 0.25 mmol) or $H^{18}OTeF_5$ by condensation of the volatile acid into the frozen solution at −196 °C. The golden red solution was thawed to 0 °C and stirred for 1 h, after which all volatiles were removed at 0 °C under vacuum. Dark purple platelets were obtained by slow evaporation of dichloromethane from a dichloromethane/heptane solution of the powder (ca. 80% yield). UV–vis (λ_{max}, nm ($10^{-3}\epsilon$, M^{-1} cm^{-1})): CH_2Cl_2, 682 (2.4), 650 (2.3), 580 (2.6), 510 (12), 408 (110); C_6H_6, 685 (3.3), 650 (3.3), 580 (4.2), 510 (16.5), 412 (114), 340 (39).

Fe(OEP)($OTeF_5$) and Fe(OEP)($^{18}OTeF_5$). A toluene solution (25 mL) of $[Fe(OEP)]_2O$ (150 mg, 0.13 mmol) was treated with a 5% excess of $HOTeF_5$ (65 mg, 0.27 mmol) or $H^{18}OTeF_5$, as above. Dark purple platelets were obtained by slow evaporation of dichloromethane from a cherry red dichloromethane/heptane solution of the powder (ca. 80% yield). UV–vis (λ_{max}, nm ($10^{-3}\epsilon$, M^{-1} cm^{-1})): CH_2Cl_2, 636 (3.8), 532 (8.8), 506 (9.5), 381 (140); C_6H_6, 636 (3.8), 532 (8.8), 506 (9.5), 381 (137).

Fe(TPP)($OTeF_5$)(THF). This compound was obtained by recrystallizing Fe(TPP)($OTeF_5$) from a minimum of tetrahydrofuran at 0 °C. UV–vis (λ_{max}, nm): THF, 690, 655 (sh), 605, 568 (sh), 525, 505, 402.

Crystallographic Study.[18] A dark purple crystal of Fe(TPP)($OTeF_5$)(THF) was centered on a Nicolet R3m diffractometer. Centering of 25 reflections (2θ(av) = 22.5°) allowed least-squares calculation of the cell constants given in Table I. This table also contains some of the details of the X-ray diffraction experiment. The intensities of three

Table I. Details of the X-ray Diffraction Study of Fe(TPP)($OTeF_5$)(THF)

chem formula	$C_{48}H_{36}N_4O_2F_5FeTe$	unit cell vol, Å^3	1025.0 (4)
		Z	1
fw	979.3	ρ_{calcd}, g cm^{-3}	1.58
space group	$P\bar{1}$	temp, °C	−130 (1)
a, Å	9.524 (3)	radiation (λ, Å)	Mo Kα (0.7107)
b, Å	11.069 (2)	μ, cm^{-1}	11.6
c, Å	11.843 (3)	transmission coeff	0.704–0.779
α, deg	102.64 (2)	R	0.0319
β, deg	104.45 (2)	R_w	0.0439
γ, deg	114.44 (2)		

(6) (a) Strauss, S. H.; Abney, K. D.; Long, K. M.; Anderson, O. P. *Inorg. Chem.* **1987**, *26*, 2638. (b) Strauss, S. H.; Noirot, M. D.; Anderson, O. P. *Inorg. Chem.* **1985**, *24*, 4307. (c) Strauss, S. H.; Noirot, M. D.; Anderson, O. P. *Inorg. Chem.* **1986**, *25*, 3850. (d) Strauss, S. H.; Colsman, M. R.; Manning, M. C.; Anderson, O. P. *Inorg. Chem.* **1987**, *26*, 3958. (e) Noirot, M. D.; Anderson, O. P.; Strauss, S. H. *Inorg. Chem.* **1987**, *26*, 2216. (f) Colsman, M. R.; Noirot, M. D.; Miller, M. M.; Anderson, O. P.; Strauss, S. H. *J. Am. Chem. Soc.* **1988**, *110*, 6886.

(7) Huppman, P.; Hartl, H.; Seppelt, K. *Z. Anorg. Allg. Chem.* **1985**, *524*, 26.

(8) Abbreviations: Por, any porphyrinate dianion; TPP, 5,10,15,20-tetraphenylporphyrinate dianion; OEP, 2,3,7,8,12,13,17,18-octaethylporphyrinate dianion; X^-, an anionic monodentate ligand, such as a halide, alkoxide, $OTeF_5^-$, perchlorate, triflate, etc.; $Hb^{III}(OH^-)$, methemoglobin hydroxide; $Mb^{III}(OH^-)$, metmyoglobin hydroxide.

(9) (a) Strauss, S. H.; Silver, M. E.; Ibers, J. A. *J. Am. Chem. Soc.* **1983**, *105*, 4108. (b) Strauss, S. H.; Silver, M. E.; Long, K. M.; Thompson, R. G.; Hudgens, R. A.; Spartalian, K.; Ibers, J. A. *J. Am. Chem. Soc.* **1985**, *107*, 4207. (c) Strauss, S. H.; Pawlik, M. J. *Inorg. Chem.* **1986**, *25*, 1921. (d) Strauss, S. H.; Thompson, R. G. *J. Inorg. Biochem.* **1986**, *27*, 173. (e) Strauss, S. H.; Long, K. M.; Magerstadt, M.; Gansow, O. A. *Inorg. Chem.* **1987**, *26*, 1185. (f) Strauss, S. H.; Pawlik, M. J.; Skowyra, J.; Kennedy, J. R.; Anderson, O. P.; Spartalian, K.; Dye, J. L. *Inorg. Chem.* **1987**, *26*, 724. (g) Pawlik, M. J.; Miller, P. K.; Sullivan, E. P., Jr.; Levstik, M. A.; Almond, D. A.; Strauss, S. H. *J. Am. Chem. Soc.* **1988**, *110*, 3007.

(10) (a) *The Porphyrins*; Dolphin, D., Ed.; Academic Press: New York, 1978: Vol. I–VII. (b) *Iron Porphyrins*; Lever, A. B. P., Gray, H. B., Eds.; Addison-Wesley: Reading, MA, 1983; Parts I and II.

(11) Shriver, D. F.; Drezdon, M. A. *The Manipulation of Air-Sensitive Compounds*, 2nd ed.; Wiley-Interscience: New York, 1986.

(12) Strauss, S. H.; Abney, K. D.; Anderson, O. P. *Inorg. Chem.* **1986**, *25*, 2806.

(13) Miller, P. K.; Abney, K. D.; Rappé, A. K.; Anderson, O. P.; Strauss, S. H. *Inorg. Chem.* **1988**, *27*, 2255.

(14) Reed, C. A.; Mashiko, T.; Bentley, S. P.; Kastner, M. E.; Scheidt, W. R.; Spartalian, K.; Lang, G. *J. Am. Chem. Soc.* **1979**, *101*, 2948.

(15) Van Geet, A. L. *Anal. Chem.* **1970**, *42*, 679.

(16) Eaton, S. S.; Eaton, G. R. *Inorg. Chem.* **1980**, *19*, 1095.

(17) Boudreaux, E. A.; Mulay, L. N. *Theory and Applications of Molecular Paramagnetism*; Wiley: New York, 1976; p 491.

(18) Calculations for diffractometer operations were performed by using software supplied with the Nicolet R3m diffractometer. All structural calculations were performed on the Data General Eclipse S/140 computer in the X-ray laboratory at Colorado State University with the SHELXTL program library written by Professor G. M. Sheldrick and supplied by Nicolet XRD Corp.

Table II. Atomic Coordinates ($\times 10^4$) and Isotropic Thermal Parameters ($Å^2 \times 10^3$)[a] for Fe(TPP)($OTeF_5$)(THF)

atom	x	y	z	U_{iso}[b]	atom	x	y	z	U_{iso}[b]
Fe′	−29 (7)	−241 (4)	−106 (5)	17 (1)*	C27	2172 (4)	2366 (4)	−2721 (3)	22 (1)*
Fe	−27 (4)	140 (3)	67 (3)	23 (1)*	C28	2873 (6)	3826 (4)	−2324 (4)	40 (2)*
Te	978 (1)	3806 (1)	1278 (1)	31 (1)*	C29	3495 (5)	4553 (4)	−3064 (4)	40 (2)*
Te′	−1030 (1)	−3920 (1)	−1316 (1)	30 (1)*	C30	3400 (5)	3815 (5)	−4204 (4)	38 (2)*
O1	306 (3)	1972 (3)	1070 (3)	32 (1)*	C31	2712 (6)	2357 (5)	−4610 (4)	38 (2)*
O2	−381 (3)	−2054 (3)	−1048 (3)	32 (1)*	C32	2102 (5)	1630 (4)	−3871 (4)	33 (2)*
N1	2281 (4)	990 (3)	−58 (3)	20 (1)*	C33	5716 (4)	1513 (4)	2769 (3)	23 (2)*
N2	−1079 (4)	175 (3)	−1618 (3)	23 (1)*	C34	6260 (5)	2451 (4)	3971 (4)	29 (2)*
N3	−2343 (4)	−1060 (3)	61 (3)	20 (2)*	C35	7890 (5)	3047 (5)	4802 (4)	37 (2)*
N4	1017	−264	1610	20 (1)*	C36	9001 (5)	2689 (4)	4437 (4)	31 (2)*
C1	3773 (5)	1349 (4)	819 (4)	22 (2)*	C37	8446 (5)	1731 (5)	3249 (4)	32 (2)*
C2	5123 (4)	2199 (4)	502 (3)	27 (2)*	C38	6802 (5)	1147 (5)	2413 (4)	27 (2)*
C3	4419 (4)	2339 (4)	−560 (4)	24 (2)*	C39	−2246 (4)	−2479 (4)	2701 (4)	24 (2)*
C4	2647 (4)	1606 (4)	−917 (3)	20 (1)*	C40	−2885 (6)	−3927 (4)	2338 (4)	42 (2)*
C5	1505 (4)	1590 (4)	−1919 (3)	21 (2)*	C41	−3502 (6)	−4645 (5)	3082 (4)	50 (2)*
C6	−251 (4)	931 (4)	−2240 (3)	21 (1)*	C42	−3494 (5)	−3932 (5)	4177 (4)	37 (2)*
C7	−1368 (4)	1030 (4)	−3200 (4)	26 (2)*	C43	−2840 (6)	−2487 (5)	4567 (5)	47 (3)*
C8	−2917 (5)	308 (4)	−3190 (4)	28 (2)*	C44	−2206 (6)	−1752 (5)	3834 (5)	42 (2)*
C9	−2759 (4)	−246 (4)	−2222 (3)	22 (1)*	F1	2338 (5)	4485 (5)	2942 (4)	50 (2)*
C10	−4054 (4)	−1036 (4)	−1882 (3)	23 (2)*	F2	2744 (7)	4067 (5)	833 (6)	88 (3)*
C11	−3863 (5)	−1420 (4)	−826 (4)	23 (2)*	F3	−659 (5)	3895 (4)	1800 (5)	58 (2)*
C12	−5184 (4)	−2290 (4)	−508 (4)	24 (2)*	F4	−269 (9)	3427 (6)	−316 (5)	94 (4)*
C13	−4506 (4)	−2468 (4)	552 (3)	24 (1)*	F5	1701 (8)	5704 (4)	1517 (5)	75 (3)*
C14	−2717 (4)	−1713 (4)	901 (3)	20 (1)*	F1′	−1747 (11)	−5789 (10)	−1484 (9)	62 (2)
C15	−1562 (4)	−1693 (4)	1915 (3)	21 (1)*	F2′	−2392 (10)	−4584 (9)	−2901 (8)	52 (2)
C16	138 (4)	−1062 (4)	2203 (3)	22 (2)*	F3′	−2814 (11)	−4154 (10)	−779 (9)	62 (2)
C17	1319 (4)	−1155 (4)	3188 (4)	28 (2)*	F4′	353 (13)	−3506 (12)	340 (11)	79 (3)
C18	2823 (4)	−416 (4)	3180 (4)	28 (2)*	F5′	571 (10)	−4033 (8)	−1863 (8)	47 (2)
C19	2647 (4)	146 (4)	2182 (3)	25 (2)*	C50′	−575 (17)	2587 (15)	668 (14)	45 (3)
C20	3978 (4)	965 (4)	1878 (3)	23 (1)*	C51′	123 (15)	4026 (12)	1556 (11)	28 (2)
C21	−5783 (4)	−1586 (4)	−2772 (3)	22 (2)*	C52′	2134 (21)	4528 (19)	2219 (18)	65 (4)
C22	−6366 (5)	−2560 (4)	−3997 (4)	29 (2)*	C53′	2015 (17)	3120 (15)	1974 (14)	46 (3)
C23	−8018 (4)	−3160 (4)	−4823 (4)	30 (2)*	C50	655 (8)	−2616 (7)	−525 (6)	32 (3)*
C24	−9058 (5)	−2769 (4)	−4432 (4)	35 (2)*	C51	−55 (10)	−4048 (8)	−1568 (8)	47 (4)*
C25	−8515 (4)	−1808 (4)	−3249 (4)	29 (2)*	C52	−1940 (10)	−4539 (10)	−2067 (11)	90 (5)*
C26	−6877 (5)	−1215 (4)	−2413 (5)	27 (2)*	C53	−2027 (8)	−3216 (7)	−1939 (8)	50 (3)*

[a] Estimated standard deviations in the least significant digits are shown in parentheses. [b] For values with asterisks, the equivalent isotropic U is defined as one-third of the trace of the U_{ij} tensor.

control reflections ($\bar{4}04$, $\bar{1}51$, $0\bar{2}6$) monitored every 97 reflections showed no trend during the course of the data collection. An empirical absorption correction, based on intensity profiles for 10 reflections over a range of setting angles (ψ) for the diffraction vector, was applied to the observed data. The transmission factor ranged from 0.704 to 0.779. Lorentz and polarization corrections were applied to the data.

The compound crystallized in a triclinic space group with $Z = 1$. The Te atoms were located by Patterson methods. Neutral atom scattering factors[19] and anomalous scattering contributions[19] were used for all atoms. Subsequent Fourier difference electron density maps (in $P1$) revealed all of the non-hydrogen atoms of [Fe(TPP)$^+$], with one teflate ion and one THF molecule as axial ligands. In addition, residual electron density above and below the porphyrin plane was observed that did not fit an ordered six-coordinate model. The pattern of this electron density indicated disorder of the teflate and THF ligands.

At this point an attempt was made to refine a centrosymmetric, disordered model in $P\bar{1}$. In the first such model, the Fe atom was fixed on an inversion center, and the asymmetric unit thus contained one teflate and one THF ligand on each side of the porphyrin plane in a 50/50 disordered fashion. In a second centrosymmetric model, the Fe atom was displaced toward the teflate anion. This model demands two possible positions for the Fe atom disposed centrosymmetrically about the center of inversion with site occupancy factors (SOF's) of 0.5 each. Refinements of these centrosymmetric models were unsuccessful as indicated by the abnormally high goodness of fit [GOF = error in an observation of unit weight = $[\sum w(|(F_o - F_c)|)^2)/(N_{data} - N_{params})]^{1/2}$] values obtained upon convergence (GOF $\geq$ 4.2, R = 0.09). Statistical analysis of the distribution of E values also supported (albeit weakly, as expected from the disordered nature of the structure) the noncentrosymmetric space group assignment (mean $|E^2 - 1|$ = 0.92 for reflections in the range (sin $\theta)/\lambda$ = 0.10–0.55; $E > 2.0$ for 2.9% of the reflections, $E > 2.5$ for 0.5% of the reflections).

The final refinement was carried out in $P1$. In this model, the teflate and THF ligands were not constrained to 50/50 disorder. Fractional iron atoms were allowed to occupy two possible iron atom positions 0.45 Å apart (based on a Fourier difference map). The SOF's for the fractional teflate and THF atoms, as well as the fractional iron atoms, were refined. The SOF's of one Fe atom and one set of THF and teflate atoms were all constrained to a single value (SOF(1)). Similarly, the complement of each of these atoms was constrained to an SOF value of 1 − SOF(1). The value of SOF(1) was refined to 0.65. The resulting disordered model can be pictured as a six-coordinate Fe(TPP)($OTeF_5$)(THF) molecule in which the teflate lies above the porphyrin plane 65% of the time and below the plane 35% of the time. Similarly, the THF moiety is disordered above and below the porphyrin plane 35% and 65% of the time, respectively. In this model, the oxygen atoms of the dissimilar major and minor ligands (e.g., major (65%) teflate and minor (35%) THF) are not resolved, resulting in an SOF of 1.00 for each oxygen atom. At an early stage of the refinement, the SOF's of the fractional Fe atoms were refined independently of the SOF's for the fractional sets of THF and teflate atoms. During this test, the SOF value for the major Fe atom and the SOF value for the major THF/teflate groups converged at 0.59. During all subsequent refinement cycles, these SOF values were constrained to be equal.

All non-hydrogen atoms, except for the minor teflate and THF moieties, were given anisotropic thermal parameters. In order to refine the minor iron atom with anisotropic thermal parameters, it was necessary to fix the distance between the major and minor iron atoms; a distance of 0.44 (1) Å was chosen on the basis of the isotropic minor Fe atom position and the anisotropic major Fe atom position. Hydrogen atoms were placed in idealized positions on the porphyrin macrocycle [C–H = 0.96 Å, U(H) = 1.2[U_{iso}(C)]].

The weighted least-squares refinement ($w = [\sigma^2(F_o) + |g|F_o^2]^{-1}$) on F converged ((shift/esd)$_{av}$ < 0.14 for the last 10 cycles) to yield the R values in Table I. In the final difference Fourier map the maximum electron density was 0.53 e Å^{-3}, positioned 0.96 Å from Te; the minimum in the map was −0.30 e Å^{-3}.

Tables II and III contain a list of atomic positional parameters and equivalent isotropic thermal parameters for all non-hydrogen atoms and a list of interatomic distances and angles for all atoms excluding the porphyrin and THF carbon atoms, respectively, for Fe(TPP)($OTeF_5$)(THF). Available as supplementary material are the complete details

(19) *International Tables for X-Ray Crystallography*; Kynoch Press: Birmingham, England, 1974: Vol. IV, pp 99, 149.

Table III. Selected Bond Lengths (Å)[a] and Angles (deg)[a] for Fe(TPP)($OTeF_5$)(THF)

Fe–Fe′	0.425 (7)	Fe–O1	1.963 (4)
Fe–N1	2.062 (5)	Fe–N2	2.014 (5)
Fe–N3	2.049 (5)	Fe–N4	2.085 (4)
Fe′–O2	1.913 (6)	Fe′–N1	2.031 (7)
Fe′–N2	2.065 (7)	Fe′–N3	2.089 (8)
Fe′–N4	2.039 (6)	Te–O1	1.794 (3)
Te–F1	1.844 (4)	Te–F2	1.817 (8)
Te–F3	1.844 (6)	Te–F4	1.809 (6)
Te–F5	1.848 (5)	Te′–O2	1.820 (3)
Te′–F1′	1.835 (11)	Te′–F2′	1.772 (8)
Te′–F3′	1.900 (12)	Te′–F4′	1.900 (12)
Te′–F5′	1.837 (10)		
O1–Fe–N1	95.0 (2)	O1–Fe–N2	96.4 (2)
N1–Fe–N2	90.6 (2)	O1–Fe–N3	95.3 (2)
N1–Fe–N3	169.4 (2)	N2–Fe–N3	90.3 (2)
O1–Fe–N4	94.6 (2)	N1–Fe–N4	87.9 (9)
N2–Fe–N4	168.9 (2)	N3–Fe–N4	89.2 (2)
O2–Fe′–N1	98.1 (3)	O2–Fe′–N2	96.6 (2)
N1–Fe′–N2	90.0 (3)	O2–Fe′–N3	95.0 (2)
N1–Fe′–N3	166.9 (3)	N2–Fe′–N3	87.8 (3)
O2–Fe′–N4	95.8 (3)	N1–Fe′–N4	90.0 (2)
N2–Fe′–N4	167.4 (3)	N3–Fe′–N4	89.3 (3)
O1–Te–F1	94.3 (2)	O1–Te–F2	94.3 (2)
F1–Te–F2	90.2 (2)	O1–Te–F3	96.1 (2)
F1–Te–F3	87.9 (2)	F2–Te–F3	169.5 (2)
O1–Te–F4	94.7 (2)	F1–Te–F4	171.0 (3)
F2–Te–F4	89.7 (3)	F3–Te–F4	90.5 (3)
O1–Te–F5	179.0 (2)	F1–Te–F5	84.8 (3)
F2–Te–F5	85.4 (3)	F3–Te–F5	84.2 (3)
F4–Te–F5	86.2 (3)	O2–Te′–F1′	175.3 (4)
O2–Te′–F2′	95.9 (3)	F1′–Te′–F2′	86.5 (4)
O2–Te′–F3′	91.7 (3)	F1′–Te′–F3′	84.3 (5)
F2′–Te′–F3′	90.8 (4)	O2–Te′–F4′	93.0 (4)
F1′–Te′–F4′	84.7 (5)	F2′–Te′–F4′	171.1 (5)
F3′–Te′–F4′	89.6 (5)	O2–Te′–F5′	98.8 (3)
F1′–Te′–F5′	85.3 (5)	F2′–Te′–F5′	88.7 (4)
F3′–Te′–F5′	169.5 (4)	F4′–Te′–F5′	89.3 (5)
Fe–O1–Te	147.4 (2)	Fe′–O2–Te′	151.7 (3)

[a] Estimated standard deviations in the least significant digits are given in parentheses.

of the X-ray crystallographic experiment (Table S-I), a complete list of bond distances and angles (Table S-II), lists of anisotropic thermal parameters (Table S-III), H atom coordinates and isotropic thermal parameters (Table S-IV), and observed and calculated structure factors (Table S-V), and a figure of the [Fe(TPP)$^+$] moiety showing the porphyrin carbon atom numbering scheme (Figure S-1). See the paragraph at the end of the paper regarding supplementary material.

Results and Discussion

Preparation and Spin State of Fe(Por)($OTeF_5$) Complexes. A wide variety of neutral five-coordinate ferric porphyrin complexes, Fe(Por)X (X$^-$ = an anionic ligand), have been prepared and characterized by using magnetic, spectroscopic, and structural measurements.[1] These complexes have a low-spin ($S = {}^1/_2$), intermediate-spin ($S = {}^3/_2$), high-spin ($S = {}^5/_2$), or quantum mechanically spin-admixed ($S = {}^3/_2, {}^5/_2$) ground state, depending on the ligand field strength of the anion. The spin state is generally discerned by magnetic susceptibility measurements and confirmed by spectroscopic data (i.e. ^{1}H NMR isotropic shifts, Mössbauer quadrupole splittings and isomer shifts, EPR g values, vibrational spectra) and structural parameters.[10,20]

The complexes Fe(TPP)($OTeF_5$) and Fe(OEP)($OTeF_5$) and their ^{18}O analogues were prepared by the protonolysis of iron(III) porphyrin μ-oxo complexes by teflic acid (eq 1). When the

$$[Fe(Por)]_2O + 2HOTeF_5 \xrightarrow[0\ °C]{\text{toluene}} H_2O + 2Fe(Por)(OTeF_5) \quad (1)$$

reaction mixture was warmed from −196 to 0 °C, an almost instantaneous color change indicated that the reaction was rapid.

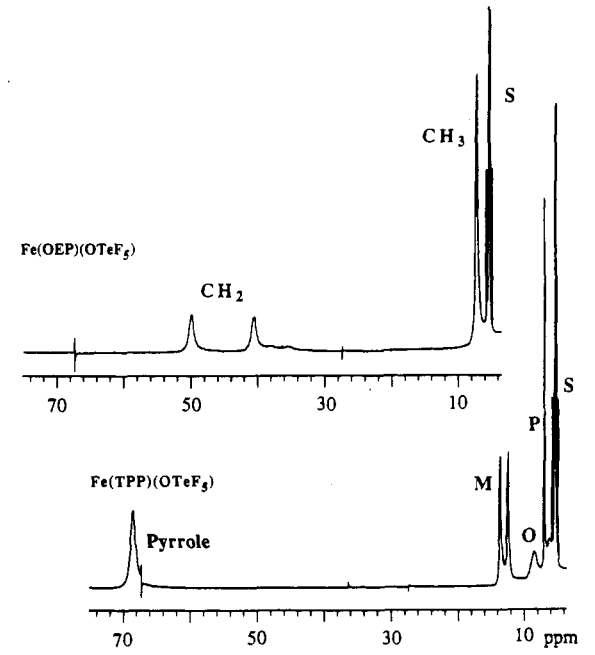

Figure 1. 200-MHz ^{1}H NMR spectra of Fe(OEP)($OTeF_5$) (CD_2Cl_2, 310 K) and Fe(TPP)($OTeF_5$) (CD_2Cl_2, 310 K). Resonances labeled, O, M, and P are phenyl group ortho, meta, and para protons, respectively. The resonance labeled S in both spectra is due to $CHDCl_2$.

Anhydrous conditions were used to avoid the rapid hydrolysis of $HOTeF_5$ to HF and *cis*-$(HO)_2TeF_4$;[21] the small concentration (~5 mM) of liberated water was not sufficient to cause hydrolysis of unreacted $HOTeF_5$. The crystalline products were stable indefinitely when stored under anhydrous conditions. The protonolysis of iron(III) porphyrin μ-oxo complexes has been used to prepare other Fe(Por)X complexes,[22] but usually with an aqueous phase present. For weakly coordinating anions such as ClO_4^-, BF_4^-, SbF_6^-, and $CF_3SO_3^-$, these preparations are more problematic due to the possible formation of $[Fe(Por)(H_2O)_2^+][X^-]$.[14] In addition, anhydrous acids of these anions are difficult to work with.

A second method used to prepare Fe(TPP)($OTeF_5$) was the metathesis reaction of Fe(TPP)Cl with $[AgOTeF_5(CH_3CN)_2]_2$ (eq 2). This reaction is analogous to that used to prepare some

$$[AgOTeF_5(CH_3CN)_2]_2 + Fe(TPP)Cl \xrightarrow[22\ °C]{CH_2Cl_2} AgCl\downarrow + Fe(TPP)(OTeF_5) + 2CH_3CN \quad (2)$$

Fe(Por)X complexes (X$^-$ = ClO_4^-, SbF_6^-, ${}^1/_2\,CrO_4^{2-}$, etc.).[14,22c,23] However, the yields from this method were not as high as those found for the protonolysis of the μ-oxo complexes.

Room-temperature magnetic susceptibility measurements were made in order to determine the spin states of the two Fe(Por)($OTeF_5$) complexes. The solid-state effective magnetic moments at 295 K were determined to be 5.9 ± 0.1 and 5.8 ± 0.1 μ_B for Fe(TPP)($OTeF_5$) and Fe(OEP)($OTeF_5$), respectively. The magnetic moments for the teflate complexes are quite close to the spin-only value of 5.92 μ_B for five unpaired electrons and to the 5.9-μ_B value found for the corresponding chloride,[24] alkoxide,[25]

(20) Scheidt, W. R.; Reed, C. A. *Chem. Rev.* **1981**, *81*, 543.

(21) Fraser, G. W.; Meikle, G. D. *J. Chem. Soc., Chem. Commun.* **1974**, 624.

(22) (a) Adler, A. D.; Iongo, F. R.; Kampas, F.; Kim, J. *J. Inorg. Nucl. Chem.* **1970**, *32*, 2443. (b) Hatano, K.; Scheidt, W. R. *Inorg. Chem.* **1979**, *18*, 877. (c) Godziela, G. M.; Ridnour, L. A.; Goff, H. M. *Inorg. Chem.* **1985**, *24*, 1610.

(23) (a) Mashiko, T.; Kastner, M. E.; Spartalian, K.; Scheidt, W. R.; Reed, C. A. *J. Am. Chem. Soc.* **1978**, *100*, 6354. (b) Goff, H.; Shimomura, E. *J. Am. Chem. Soc.* **1980**, *102*, 31. (c) Masuda, H.; Taga, T.; Osaki, K.; Sugimoto, H.; Yoshida, A.-I.; Ogoshi, H. *Inorg. Chem.* **1980**, *19*, 950. (d) Shelly, K.; Bartczak, T.; Scheidt, W. R.; Reed, C. A. *Inorg. Chem.* **1985**, *24*, 4325. (e) Shelly, K.; Reed, C. A.; Lee, Y. J.; Scheidt, W. R. *J. Am. Chem. Soc.* **1986**, *108*, 3117.

Table IV. Mid- and Far-Infrared Spectral Data (cm^{-1}) for $Fe(TPP)(OTeF_5)$ and $Fe(OEP)(OTeF_5)$[a]

	$Fe(TPP)(OTeF_5)$	$Fe(OEP)(OTeF_5)$
ν(TeO)	849 (~806)[b]	852 (812)
$\nu(TeF_4)_{asym}$	680 (680)	682 (682)
ν(FeO)	423 (~410)	415 (402)
ν(FeN) + porphyrin bands	330, 279 (329, 318, 279)[c]	281, 257 (281, 258)[d] 336, 331, 326 (336, 331, 325, 313)

[a] Solid-state spectra at 22 °C. Values in parentheses are for the ^{18}O-substituted derivatives. [b] Substitution of ^{18}O results in a band for $\nu(Te^{18}O)$ that overlaps a porphyrin band at 806 cm^{-1}. [c] ν(FeN) + porphyrin ring deformations. [d] ν(FeN).

and carboxylate complexes.[26] In addition, these values are much higher than the spin-only value of 3.87 μ_B for three unpaired electrons and the 4.1–5.4 μ_B found for complexes with spin-admixed ($S = {}^3/_2, {}^5/_2$) ground states.[14,23c,d,27-30]

The ^1H NMR spectra of both complexes are shown in Figure 1. The pyrrole proton resonance for $Fe(TPP)(OTeF_5)$ at 72.3 ppm (290 K) lies within the range of 72–75 ppm found for the pyrrole resonance in other high-spin oxyanionic complexes.[31] This value is much further downfield than the values of 13–50 ppm found for spin-admixed ($S = {}^3/_2, {}^5/_2$) oxyanionic complexes such as $Fe(TPP)(ClO_4)$ and $Fe(TPP)(CF_3SO_3)$.[31c,32] For $Fe(OEP)(OTeF_5)$ the two methylene proton resonances (55.3 and 44.5 ppm; 300 K) are further downfield than the corresponding resonances for high-spin Fe(OEP)Cl (44.1 and 39.5 ppm; 302 K).[33] The methylene proton resonances for the perchlorate and triflate complexes appear from 34.6 to 49.4 ppm (302 K).[31c,32] The meso proton resonance at −40 ppm for $Fe(OEP)(OTeF_5)$ is near the value found for high-spin iron(III) complexes (−50 ppm) and upfield of the range (−5 to −25 ppm) found for spin-admixed iron(III) porphyrin complexes.[31c]

The variable-temperature data for $Fe(TPP)(OTeF_5)$ and $Fe(OEP)(OTeF_5)$ approximate Curie behavior. Plots of pyrrole and phenyl shifts (δ) for the TPP complex and methylene and methyl shifts (δ) for the OEP complex vs $1/T$ show a linear relationship with deviations of the $1/T = 0$ intercepts from diamagnetic values close to those found for the analogous chloride complexes.[34] The variable-temperature ^1H NMR spectra of high-spin iron(III) porphyrin complexes have been well studied.[33,35] For these complexes, departure from linearity of a Curie plot arises from the $1/T^2$ dependence of the dipolar contribution to the isotropic shift. The magnitude of the dipolar contribution is a function of the zero-field splitting (ZFS), which varies with the axial ligand. For complexes with a large ZFS, such as Fe(TPP)I, the Curie plot will show pronounced curvature. For complexes with a smaller ZFS, such as Fe(TPP)Cl, the plot will be essentially linear over the temperature range accessible with common NMR solvents.[36] Thus, magnetic susceptibility and variable-temperature ^1H NMR results allow the assignment of a high-spin state to the iron(III) ion in $Fe(TPP)(OTeF_5)$ and $Fe(OEP)(OTeF_5)$, and the NMR data indicate that $OTeF_5^-$ induces a ZFS of about the same magnitude as does chloride.

Table V. Infrared Data for Representative $OTeF_5$ Compounds

compd	ν(TeO),[a] cm^{-1}
$B(OTeF_5)_3$	<740[b]
$HOTeF_5$	734[c]
$Pt(OTeF_5)_2(NBD)$	816[d,e]
$Mn(CO)_5(OTeF_5)$	848[f]
$Fe(TPP)(OTeF_5)$	849 (CH_2Cl_2, 848)
$Fe(TPP)(OTeF_5)(THF)$	844 (THF, 847[g])
$Fe(OEP)(OTeF_5)$	852 (CH_2Cl_2, 852)
$[N(n\text{-}Bu)_4^+][OTeF_5^-]$	867[h] (CH_2Cl_2, 861;[h] THF, 861[i])

[a] Solid-state IR data unless otherwise noted; all data from this work unless otherwise noted. [b] Highest energy band attributable to ν(TeO) or ν(TeF): Kropshofer, H.; Leitzke, O.; Peringer, P.; Sladky, F. *Z. Anorg. Allg. Chem.* **1973**, *399*, 65. [c] Gas-phase spectrum; this single band is a combination of ν(TeO) and ν(TeF): Burger, H. *Z. Anorg. Allg. Chem.* **1968**, *360*, 97. [d] Reference 6d; NBD = norbornadiene. [e] Average of two observed IR bands, 805 and 827 cm^{-1}. [f] Reference 6a. [g] Extrapolation of $\nu(Te^{18}O) = 806$ cm^{-1} for $Fe(TPP)(^{18}OTeF_5)$ in THF using the equation $\nu(Te^{16}O) = (1.051)(\nu(Te^{18}O))$. [h] References 12 and 13. [i] Extrapolation of $\nu(Te^{18}O) = 819$ cm^{-1} for $[N(n\text{-}Bu)_4^+][^{18}OTeF_5^-]$ in THF using the equation from footnote *g*.

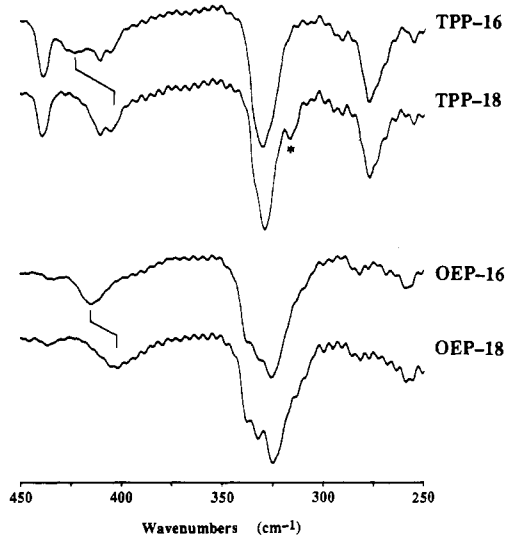

Figure 2. Far-infrared spectra of the ^{16}O and ^{18}O equivalents of $Fe(TPP)(OTeF_5)$ and $Fe(OEP)(OTeF_5)$. The band marked by an asterisk appears upon ^{18}O substitution into $Fe(TPP)(OTeF_5)$.

Attempts were made to locate the ^{19}F NMR resonances expected for the teflate group in $Fe(TPP)(OTeF_5)$ using a 100-kHz spectral width centered near 0 ppm. No signal was observed, perhaps due to paramagnetic broadening of the expected AB_4 pattern. The AB_4 pattern for the fluorine resonances for $[N(n\text{-}Bu)_4^+][OTeF_5^-]$ in CD_2Cl_2 are found at −19 ppm for δ_A and −36.8 ppm for δ_B.[12] The ^{19}F NMR spectrum of $Fe(TPP)(SO_3CF_3)$ has been recorded,[31c] and the resonance occurs as a broad (~5 ppm) singlet at −19 ppm, which is 60 ppm downfield of the fluorine resonance for $[N(n\text{-}Bu)_4^+][SO_3CF_3^-]$. However, ^{19}F NMR data have not been reported for the axial ligand for any high-spin five-coordinate iron(III) porphyrin complex.

Nature of the Fe–$OTeF_5$ Bond. Information about the Fe–O bonds in the $Fe(Por)(OTeF_5)$ complexes can be obtained from vibrational spectroscopy. The mid-infrared spectra of $Fe(OEP)(OTeF_5)$ and $Fe(TPP)(OTeF_5)$ and their ^{18}O derivatives are summarized in Table IV. The spectrum of the natural-abundance OEP complex shows a band at 852 cm^{-1}, which shifts to 812 cm^{-1} upon ^{18}O substitution. The TPP complex shows a feature at 849 cm^{-1}, which shifts to overlap a porphyrin band at 806 cm^{-1} upon ^{18}O substitution. These bands are assigned to ν(TeO), and the strong bands at 680 and 682 cm^{-1} for the TPP and OEP complexes, respectively, are assigned to $\nu(TeF_4)_{asym}$.[13]

(24) Maricondi, C.; Swift, W.; Straub, D. K. *J. Am. Chem. Soc.* **1969**, *91*, 5205.
(25) Tang, S. C.; Koch, S.; Pagaefthymiou, G. C.; Foner, S.; Frankel, R. B.; Ibers, J. A.; Holm, R. H. *J. Am. Chem. Soc.* **1976**, *98*, 2414.
(26) Oumous, H.; Lecomte, C.; Protas, J.; Cocolios, P.; Guilard, R. *Polyhedron*, **1984**, *3*, 651.
(27) Kastner, M. E.; Scheidt, W. R.; Mashiko, T.; Reed, C. A. *J. Am. Chem. Soc.* **1978**, *100*, 666.
(28) Dolphin, D. H.; Sams, J. R.; Tsin, T. B. *Inorg. Chem.* **1977**, *16*, 711.
(29) Summerville, D. A.; Cohen, I. A.; Hatano, K.; Scheidt, W. R. *Inorg. Chem.* **1978**, *17*, 2906.
(30) Gupta, G. P.; Lang, G.; Lee, Y. J.; Scheidt, W. R.; Shelly, K.; Reed, C. A. *Inorg. Chem.* **1987**, *26*, 3022.
(31) (a) Godziela, G. M.; Ridnour, L. A.; Goff, H. M. *Inorg. Chem.* **1985**, *24*, 1610. (b) Phillippi, M. A.; Baenziger, N.; Goff, H. M. *Inorg. Chem.* **1981**, *12*, 3904. (c) Boersma, A. D.; Goff, H. M. *Inorg. Chem.* **1982**, *21*, 581.
(32) Goff, H. M.; Shimomura, E. *J. Am. Chem. Soc.* **1980**, *102*, 31.
(33) Walker, F. A.; LaMar, G. N. *Ann. N.Y. Acad. Sci.* **1973**, *206*, 328.
(34) Slopes and intercepts from linear least-squares fits to the data are given in the supplementary material, Table S-VI.
(35) LaMar, G. N.; Eaton, G. E.; Walker, F. A.; Holm, R. H. *J. Am. Chem. Soc.* **1973**, *95*, 63.
(36) Behere, D. V.; Birdy, R.; Mitra, S. *Inorg. Chem.* **1982**, *21*, 386 and references therein.

As has been discussed,[6,12,13] ν(TeO) is sensitive to the "degree of ionicity of the teflate group", ranging from 733 and 740 cm^{-1} for covalently bonded teflates such as $HOTeF_5$[37] and $B(OTeF_5)_3$,[3] respectively, to 867 cm^{-1} for an ionic teflate such as $[N(n\text{-}Bu)_4^+][OTeF_5^-]$[12,13] (Table V). The TeO stretching frequencies of both Fe(TPP)($OTeF_5$) and Fe(OEP)($OTeF_5$) indicate that the complexes contain teflate groups that are quite ionic. Therefore, as would be expected for high-spin iron(III) complexes, the Fe–O bond has a large degree of ionic character. The M–O bonds in other transition-metal teflate complexes have also been found to have a large ionic component, as indicated by their TeO stretching frequencies (Table V).

Far-infrared spectra are shown in Figure 2 and are summarized in Table IV. The spectrum of the natural-abundance OEP complex clearly shows a band at 415 cm^{-1}, which shifts to 402 cm^{-1} upon ^{18}O substitution. The spectrum for the TPP complex is more complicated in this region but shows a feature at 423 cm^{-1} (^{16}O) that shifts to ~410 cm^{-1} (^{18}O). These bands are assigned to ν(FeO) and compare favorably with ν(FeO) values of 530–540 cm^{-1} for Fe(Por)(OMe) complexes,[38,39] 530–588 cm^{-1} for Fe(Por)(O_2CR) complexes,[26] and 495 and 490 cm^{-1} reported for $Hb^{III}(OH^-)$[40,41] and $Mb^{III}(OH^-)$,[41,42] respectively.[8] The FeO stretching frequencies for the $OTeF_5^-$ complexes are lower than even the protein values, despite the expectation that a five-coordinate complex would have a stronger Fe–O bond than a six-coordinate complex. However, $OTeF_5^-$ is a weaker Lewis base than Cl^-[6a] and, presumably, hydroxide, methoxide, and carboxylates, and so the FeO stretching frequency should be lower for analogous $OTeF_5^-$ complexes. Although the bond is not as strong as those found for the other iron(III) porphyrin oxyanionic complexes mentioned above, the Fe–$OTeF_5$ bond is not readily cleaved even by the coordinating solvent THF (see below). Thus, the values of ν(TeO) and ν(FeO) are consistent with a relatively strong but ionic Fe–O bond.

For both porphyrins, several bands observed below 400 cm^{-1} have been assigned to Fe–N stretches and porphyrin vibrational modes (Table IV). The iron–nitrogen stretches in Fe(OEP)($OTeF_5$) at 281 and 257 cm^{-1} are consistent with the values found by Ogoshi et al.[43] for other five-coordinate high-spin complexes, which ranged from 250 to 280 cm^{-1}. In addition, the observation of two stretches is indicative of C_{4v} symmetry with the Fe atom substantially above the mean nitrogen plane.[43]

A medium-intensity band appears at 439 cm^{-1} in the far-IR spectrum of Fe(TPP)($OTeF_5$) and can be assigned to a low-energy porphyrin core deformation mode in analogy to the assignment made by Nakamoto et al.[44] This spin-state-sensitive band appears only at a slightly higher energy than the 432–435-cm^{-1} range observed by Nakamoto for other high-spin Fe(TPP)X complexes. However, the value is not as high as that found for spin-admixed Fe(TPP)(ClO_4) (447 cm^{-1}).

Both complexes exhibit the expected shifts in ν(TeO) and ν(FeO) upon ^{18}O substitution (Table IV). However, the ratio $\nu(Fe^{16}O)/\nu(Fe^{18}O)$ of 1.032 for Fe(OEP)($OTeF_5$) is lower than the predicted value of 1.046 for a simple Fe–O oscillator. This may be due to partial mixing of ν(FeO) and porphyrin vibrations. Such mixing of iron–axial ligand stretching normal modes with porphyrin vibrations has been observed by others.[45] Note that the region around 325 cm^{-1} shows consistent changes for both the OEP and TPP complexes upon isotopic substitution, with a lower energy band or shoulder appearing for the ^{18}O derivatives at about 315 cm^{-1}. These changes are more apparent for the TPP complex. Bands in this region have been assigned to ν(FeN) as well as to a mixture of Fe–N and porphyrin core in-plane bending modes.[43,46] Alternatively, a band due to a Te–O–Fe bending mode could overlap the ν(FeN) and porphyrin bands that occur in this region.

Structure of Fe(TPP)($OTeF_5$)(THF). When Fe(TPP)($OTeF_5$) is dissolved in the coordinating solvent THF, the formation of $[Fe(TPP)(THF)_2^+][OTeF_5^-]$ does not occur. This was demonstrated by the solution IR spectrum of Fe(TPP)($^{18}OTeF_5$) in THF, which displays a $Te^{18}O$ stretch at 806 cm^{-1} and a TeF_4 asymmetric stretch at 677 cm^{-1}. The solution IR spectrum of $[N(n\text{-}Bu)_4^+][^{18}OTeF_5^-]$ in THF has $\nu(Te^{18}O)$ at 819 cm^{-1} and $\nu(TeF_4)_{asym}$ at 640 cm^{-1}. These data suggest that the equilibrium constant, β_2, is much less than 1 for reaction 3. It was not possible

$$Fe(TPP)(OTeF_5) + 2THF \underset{}{\overset{\beta_2 \ll 1}{\rightleftharpoons}} [Fe(TPP)(THF)_2^+][OTeF_5^-] \quad (3)$$

$$\beta_2 = \frac{[[Fe(TPP)(THF)_2^+]][[OTeF_5^-]]}{[Fe(TPP)(OTeF_5)][THF]^2}$$

to observe $\nu(Te^{16}O)$ for Fe(TPP)($^{16}OTeF_5$) in THF solution because of a solvent absorption from ~970 to ~830 cm^{-1}. An estimated value of $\nu(Te^{16}O)$ of 847 cm^{-1} for Fe(TPP)($OTeF_5$) in THF may be calculated from the expected isotope shift: (806 cm^{-1})(1.051) = 847 cm^{-1}, where 1.051 = $\nu(Te^{16}O)/\nu(Te^{18}O)$ for $[N(n\text{-}Bu)_4^+][OTeF_5^-]$ in the solid-state.[13] (The calculated $\nu(Te^{16}O)$ value for $[N(n\text{-}Bu)_4^+][OTeF_5^-]$ in THF is 861 cm^{-1} (cf. CH_2Cl_2, 861 cm^{-1})). The solid-state IR spectrum of the six-coordinate mixed-ligand complex Fe(TPP)($OTeF_5$)(THF), described below, shows ν(TeO) at 844 cm^{-1} (Table V). The THF ligand readily evaporates from crystals of this compound, as evidenced by the disappearance of the band at 844 cm^{-1} and the concomitant appearance of the ν(TeO) band for Fe(TPP)($OTeF_5$) at 849 cm^{-1} in solid-state IR spectra.

In contrast to this behavior, Fe(OEP)(ClO_4) forms the bis THF adduct $[Fe(OEP)(THF)_2^+][ClO_4^-]$[47] when dissolved in THF. This salt has been structurally characterized by Masuda et al.[48] Goff et al.[23b] have observed the broadening of THF proton NMR resonances for a chloroform-*d* solution of Fe(TPP)(ClO_4) containing 2 equiv of THF, suggesting rapid THF exchange with bound THF molecules. It is possible that, in Goff's experiment, the mixed-ligand complex Fe(TPP)(ClO_4)(THF) is formed to some extent.

The compound Fe(TPP)($OTeF_5$)(THF) was isolated from a neat THF solution of Fe(TPP)($OTeF_5$). To establish the THF/Fe stoichiometry, a known amount of Me_4Si and Fe(TPP)($OTeF_5$)(THF) crystals were stirred in dichloromethane-d_2. A ^1H NMR spectrum of the volatiles from this solution indicated the presence of one THF molecule for each Fe(TPP)($OTeF_5$). This result rules out the possibility of a species such as $[Fe(TPP)(THF)_2^+][OTeF_5^-]$ in the crystal structure. It also rules out any significant amount of five-coordinate Fe(TPP)($OTeF_5$) mixed in with Fe(TPP)($OTeF_5$)(THF). The structural results confirm that Fe(TPP)($OTeF_5$)(THF) is a six-coordinate molecule with axial $OTeF_5^-$ and THF ligands. The oxygen atoms of the dissimilar major and minor axial ligands were not resolved (see Experimental Section for a discussion of how the crystalline disorder for this compound was modeled). Resolution of the major and minor atoms of the porphyrin ring was not attempted, due to the small magnitude of the expected differences. We feel that the differences between the major and minor bond distances for the $OTeF_5^-$ and THF ligands are the result of a less than perfect model for the disorder present in the structure and that the limitations in that model probably have resulted in estimated standard deviations that are significantly underestimated. We see no reason to assume

(37) Burger, H. *Z. Anorg. Allg. Chem.* **1968**, *360*, 97.
(38) Sadavisan, N.; Eberpaecher, H. I.; Fuchsman, W. H.; Caughey, W. S. *Biochemistry* **1969**, *8*, 534.
(39) Buchler, J. W.; Puppe, L.; Rohbock, K.; Schneehage, H. H. *Chem. Ber.* **1973**, *106*, 2710.
(40) Asher, S. A.; Vickery, L. E.; Schuster, T. M.; Sauer, K. *Biochemistry* **1977**, *16*, 5849.
(41) Asher, S. A.; Schuster, T. M. *Biochemistry* **1979**, *18*, 5377.
(42) Desbois, A.; Lutz, M.; Banerjee, R. *Biochemistry* **1979**, *18*, 1510.
(43) Ogoshi, H.; Watanabe, E.; Yoshida, A.; Kincaid, J.; Nakamoto, K. *J. Am. Chem. Soc.* **1973**, *95*, 2845.
(44) Oshio, H.; Ama, T.; Watanabe, T.; Kincaid, J.; Nakamoto, K. *Spectrochim. Acta* **1984**, *40A*, 863.
(45) Crisanti, M. A.; Spiro, T. G.; English, D. R.; Hendrickson, D. N.; Suslick, K. S. *Inorg. Chem.* **1984**, *23*, 3897.
(46) Kincaid, J.; Nakamoto, K. *J. Inorg. Nucl. Chem.* **1975**, *37*, 85.
(47) Ogoshi, H.; Sugimoto, H.; Watanabe, E.; Yoshida, Z.; Maeda, Y.; Sakai, H. *Bull. Chem. Soc. Jpn.* **1981**, *54*, 3414.
(48) Masuda, H.; Taga, T.; Osaki, K.; Sugimoto, H.; Yoshida, Z.; Ogoshi, H. *Bull. Chem. Soc. Jpn.* **1982**, *55*, 3891.

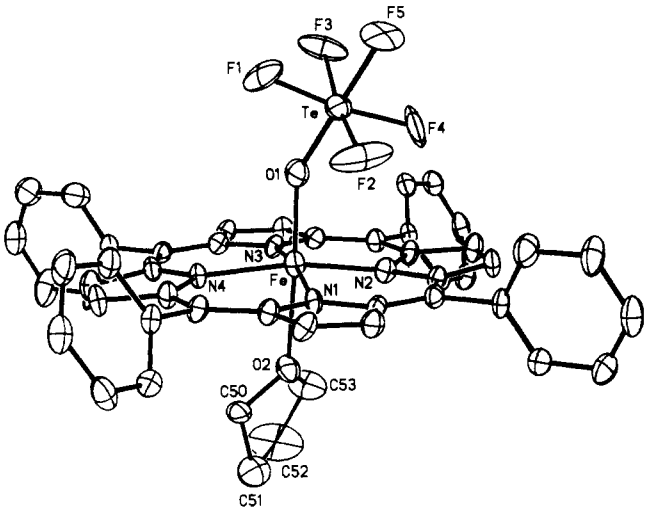

Figure 3. Drawing of the Fe(TPP)($OTeF_5$)(THF) molecule (50% ellipsoids) showing the major component (65%) atoms. Hydrogen atoms have been omitted for clarity.

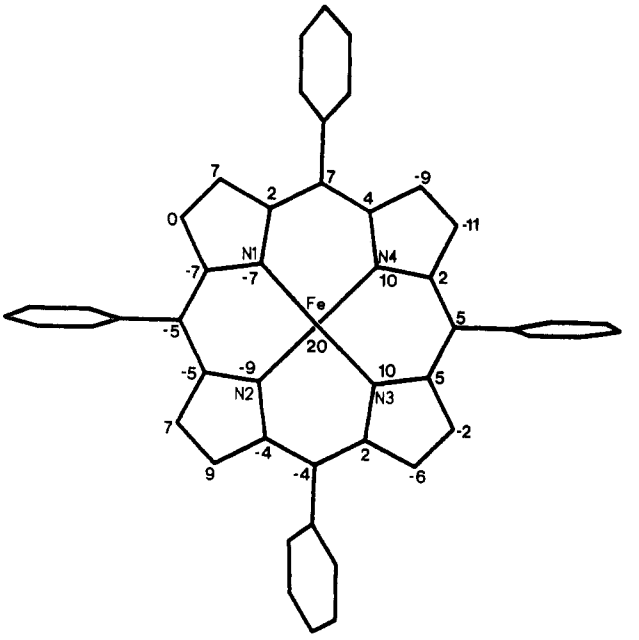

Figure 4. Out-of-plane displacements (in units of 0.01 Å) for the Fe(TPP)$^+$ fragment of Fe(TPP)($OTeF_5$)(THF). The plane is defined as the best least-squares plane of the 24 atoms of the porphyrin core. Positive displacements are defined as being in the direction of the major $OTeF_5^-$. The estimated standard deviation for each value is 0.01 Å.

that the major and minor ligands are truly different. For the purposes of the following discussion, the values of the major component bond distances and angles will be used.

A drawing of the unsymmetrically ligated Fe(TPP)($OTeF_5$)(THF) molecule is shown in Figure 3, which is drawn without the minor component (35%) atoms or hydrogen atoms for clarity. The Fe–N_p distances, which range from 2.014 to 2.085 Å, leave little doubt that the Fe(III) ion is high-spin in Fe(TPP)($OTeF_5$)(THF), since these distances are much longer than the range of 1.97–2.00 Å found for low-spin ferric porphyrins.[20] Furthermore, the average Fe–N_p bond distance of 2.05 (3) Å is close to the average value of 2.048 (4) Å observed for the only other structurally characterized, unsymmetrically substituted, high-spin ferric porphyrin, Fe(OEP)(NCS)(py).[49] Figure 4 displays the out-of-plane displacements for the Fe(TPP)$^+$ fragment with positive values representing displacements toward the major component teflate ligand. Although caution must be taken in drawing conclusions from this diagram due to the unresolved disorder in the porphyrin core, the displacements are consistent with expansion of the core by a C_i distortion in which two adjacent pyrroles tip upward and two downward. This expansion has been observed for other six-coordinate high-spin iron(III) porphyrins.[23a,50] The iron atom is displaced 0.20 Å from the mean 24-atom porphyrin plane toward the teflate anion. This result is analogous to that found for Fe(OEP)(NCS)(py), in which the iron atom is displaced 0.24 Å from the mean porphyrin plane toward the anionic isothiocyanate ligand.[49]

The Fe–O1($OTeF_5$) bond distance of 1.967 (5) Å is considerably longer than the 1.82–1.90-Å distances found for five-coordinate ferric porphyrins with the axial oxyanion ligands OCH_3^-,[51,52] $CH_3CO_2^-$,[26] and SO_4^{2-}.[53] However, the Fe–O1($OTeF_5$) distance is shorter than the Fe–O distances seen in Fe(TPP)($OClO_3$) (2.094 (4) Å)[14] and Fe(OEP)($OClO_3$) (2.067 (9) Å).[23c] It is also shorter than the 2.07–2.10-Å distances found for axially symmetric, six-coordinate, high-spin ferric porphyrin complexes with the neutral oxygen donors $(CH_2)_4SO$[23a] and H_2O.[50] The Fe–O2(THF) distance of 2.334 (7) Å (obtained by addition of the Fe–Fe′ vector to the Fe′–O2 vector) is significantly longer than not only the Fe–O distances observed for the high-spin $(CH_2)_4SO$ and H_2O cationic complexes but also the 2.19 (1) Å Fe–O distance in the intermediate-spin complex [Fe(TPP)$(THF)_2^+$][ClO_4^-].[48] The short Fe–O1($OTeF_5$) distance and the displacement of the iron atom toward the teflate are consistent with a much stronger metal–ligand bond to the teflate anion than to the THF molecule. This type of asymmetry in bond strengths was also observed for Fe(OEP)(NCS)(py) (Fe–N(NCS) = 2.031 (2) Å, Fe–N(py) = 2.442 (2) Å).[49]

The relatively short Te–O bond distance of 1.793 (4) Å in Fe(TPP)($OTeF_5$)(THF) indicates a strong Te–O bond and a teflate group possessing a large degree of ionic character. As discussed in previous papers,[6,12,13] short Te–O bond distances for ionic teflate groups arise from either O→Te p–d π-bonding or an electrostatic interaction between the oxygen and tellurium atoms. The bond weakens and lengthens as the teflate anion becomes ion-paired or covalently bonded to another atom, so short Te–O bond distances and high TeO stretching frequencies (see Table V) can be correlated with a large amount of ionic character for the teflate group. The Te–F bond distances and the bond angles in the teflate group are normal when compared to those in other structurally characterized teflate compounds.[6,7,12,13,54] The oxygen and fluorine atoms exhibit large-amplitude thermal motion (Tables II and S-I), but this is well within the range of thermal motion exhibited in other teflate structures.[6,7,12,13,54]

The Te–O1–Fe angle is 147.3 (3)°. The range found for the other structurally characterized metal–teflate compounds is 123–180°.[6,7,54] The Te–O1–Fe–N1 torsion angle is 46.7°. The Te–O bond projection onto the porphyrin plane almost bisects the N1–Fe–N2 angle, while the projections of the Te–F2 and Te–F4 bonds roughly parallel the Fe–N1 and Fe–N2 bonds, respectively. The closest contact between the teflate fluorine atoms and the porphyrin ring are F2···C4 (2.991 Å), F2···N1 (3.139 Å), F4···C6 (3.183 Å), and F4···N2 (3.258 Å). These contacts may represent steric effects that would cause the Fe–O1–Te angle to be larger than if unconstrained. The two Fe–O bonds are nearly collinear (O1–Fe–O2 = 177.6°). The relative disposition of the axial ligands can best be described by using the dihedral angles defined by the Te–O1–O2 plane with the O1–O2–C50 plane (110.1°) and

(49) Scheidt, W. R.; Lee, Y. J.; Geiger, D. K.; Taylor, K.; Hatano, K. *J. Am. Chem. Soc.* **1982**, *104*, 3367.
(50) Scheidt, W. R.; Cohen, I. A.; Kastner, M. E. *Biochemistry* **1979**, *18*, 3546.
(51) Hoard, J. L.; Hamor, M. J.; Hamor, T. A.; Caughey, W. S. *J. Am. Chem. Soc.* **1965**, *87*, 2312.
(52) Lecomte, C.; Chadwick, D. L.; Coppens, P.; Stevens, E. D. *Inorg. Chem.* **1983**, *22*, 2982.
(53) Scheidt, W. R.; Lee, Y. J.; Bartzcak, T.; Hatano, K. *Inorg. Chem.* **1984**, *23*, 2552.
(54) (a) Templeton, L. K.; Templeton, D. H.; Bartlett, N.; Seppelt, K. *Inorg. Chem.* **1976**, *15*, 2720. (b) Huppmann, V. P.; Labischinski, H.; Lentz, D.; Pritzkow, H.; Seppelt, K. *Z. Anorg. Allg. Chem.* **1982**, *487*, 7.

with the O1–O2–C53 plane (102.3°). The staggering of the axial ligands indicated by these dihedral angles may prevent severe nonbonded contacts with the porphyrin core.

Comparison of $OTeF_5^-$ to Other Anionic Ligands. A cyclic voltammogram (CV) background scan of $[N(n\text{-}Bu)_4^+][OTeF_5^-]$ in dichloromethane was essentially flat from +2.5 to −1.5 V (SCE). When $Fe(TPP)(ClO_4)$ was added to this solution, the CV showed an irreversible reduction at −0.16 V (Fe(III)/Fe(II)). Since the reduction of $Fe(TPP)(ClO_4)$ has been reported to occur at +0.14[55] and +0.22 V[56] in dichloromethane containing 0.10 M $[N(n\text{-}Bu)_4^+][ClO_4^-]$, replacement of ClO_4^- by $OTeF_5^-$ must have occurred. CV's of $Fe(TPP)(OTeF_5)$ in 0.1 M $[N(n\text{-}Bu)_4^+][OTeF_5^-]$ were measured in dichloromethane and showed the same irreversible reduction at −0.16 V. Since the −0.16-V value is anodic of the values found for high-spin Fe(III) halides[56] but cathodic of those for ClO_4^- and $CF_3SO_3^-$[31c] complexes, teflate lies between the halides and the weak ligands perchlorate and triflate in ligand-binding character.[56] The first oxidation of $Fe(TPP)(OTeF_5)$ appears as a quasi-reversible wave with a half-wave potential of 1.01 V. This value compares favorably with the half-wave potentials of 1.08–1.11 V found for the first oxidation of five-coordinate Fe(III) porphyrins.[55,57] The cathodic value of the potential is indicative of ring oxidation instead of metal-centered oxidation (cf. $Fe(TPP)F_2^-$, $E_{1/2}$ = 0.68 V for Fe(III)/Fe(IV)[58]).

Ligand displacement reactions were investigated by solution infrared spectroscopy to further confirm the ligand-binding strength of teflate relative to that of chloride and perchlorate. When 1 equiv of $N(n\text{-}Bu)_4^+Cl^-$ was added to a dichloromethane solution of $Fe(TPP)(OTeF_5)$, the complete displacement of teflate by chloride was indicated by the disappearance of the 848-cm^{-1} ν(TeO) band and the appearance of an 861-cm^{-1} band for the TeO stretch of free, ionic teflate.[12] Likewise, the complete displacement of ClO_4^- by $OTeF_5^-$ upon addition of $[N(n\text{-}Bu)_4^+][OTeF_5^-]$ to a dichloromethane solution of $Fe(TPP)(ClO_4)$ was shown by the disappearance of the 861-cm^{-1} band for free teflate and the appearance of ν(TeO) at 848-cm^{-1} for $Fe(TPP)(OTeF_5)$ and a free perchlorate band at 624-cm^{-1} (asymmetric bend).[59] Since it is known that Cl^- will displace ClO_4^- in $Fe(Por)(ClO_4)$ complexes,[60] the ligand displacement reactions confirm the ligand-binding strengths found electrochemically, $Cl^- > OTeF_5^- > ClO_4^-$.

Summary and Conclusions. This study has shown that $OTeF_5^-$ forms high-spin $Fe(Por)(OTeF_5)$ and $Fe(TPP)(OTeF_5)(THF)$ complexes. The iron–teflate bonds are moderately strong with a large component of ionic character, and the ligand binding strength of teflate follows the order $Cl^- > OTeF_5^- > ClO_4^-$. The electronic and steric differences between teflate and other weakly basic oxyanions such as perchlorate and triflate suggest that teflate may be a useful ligand for highly reactive complexes, where a small change in ligand properties can produce dramatic differences in reactivity.

Acknowledgment. This research was supported by grants from the National Science Foundation (CHE-8419719) and the National Institutes of Health (GM 31554). We thank Professor J. R. Norton for the use of his IR spectrometer and J. H. Reibenspies and M. M. Miller for experimental assistance. P.J.K. thanks the Mobay Corp. for a Graduate Student Research Award. The Nicolet R3m/E diffractometer and computing system was purchased with a grant from the NSF (CHE-8103011).

Registry No. $[AgOTeF_5(CH_3CN)_2]_2$, 98330-70-2; $[Fe(TPP)]_2O$, 12582-61-5; $[Fe(OEP)]_2O$, 39393-88-9; $Fe(TPP)(ClO_4)$, 59370-87-5; $Fe(TPP)(OTeF_5)$, 113704-01-1; $Fe(TPP)(^{18}OTeF_5)$, 118207-88-8; $Fe(OEP)(OTeF_5)$, 113704-02-2; $Fe(OEP)(^{18}OTeF_5)$, 118207-89-9; $Fe(TPP)(OTeF_5)(THF)$, 118207-90-2; Fe(TPP)Cl, 16456-81-8.

Supplementary Material Available: Numbering scheme of the $Fe(TPP)^+$ moiety of $Fe(TPP)(OTeF_5)(THF)$ (Figure S1), a complete listing of the details of the X-ray crystallographic experiment (Table S-I), a complete listing of interatomic distances and angles (Table S-II), a listing of anisotropic thermal parameters for all non-hydrogen atoms (Table S-III), a table of hydrogen atom positions and isotropic thermal parameters (Table S-IV), and a table of linear least-squares parameters for δ versus $1/T$ plots for $Fe(TPP)(OTeF_5)$ and $Fe(OEP)(OTeF_5)$ (Table S-VI) (13 pages); a table of observed and calculated structure factors (Table S-V) (25 pages). Ordering information is given on any current masthead page.

(55) Phillippi, M. A.; Shimomura, E. T.; Goff, H. M. *Inorg. Chem.* **1981**, *20*, 1322.
(56) Bottomley, L. A.; Kadish, K. M. *Inorg. Chem.* **1981**, *20*, 1348.
(57) Kadish, K. M.; Bottomley, L. A. *Inorg. Chem.* **1980**, *19*, 832.
(58) Hickman, D. L.; Goff, H. M. *Inorg. Chem.* **1983**, *22*, 2789.
(59) Gowda, N. M. N.; Naikar, S. B.; Reddy, G. K. N. *Adv. Inorg. Chem. Radiochem.* **1984**, *28*, 255.
(60) In ref 57, Kadish et al. calculated K_{ex} = 10.3 for the reaction $Fe(TPP)(ClO_4) + Cl^- \rightleftharpoons Fe(TPP)Cl + ClO_4^-$; however, no $Fe(OEP)(ClO_4)$ was detected by cyclic voltammetry in the reaction of $Fe(OEP)(ClO_4)$ with 1 equiv of Cl^-.

Contribution from the Department of Chemistry, Faculty of Science, Tohoku University, Aoba, Aramaki, Sendai 980, Japan

(μ-Ethylenediaminetetraacetato)(μ-oxo)(μ-sulfido)bis(oxotungstate(V)): The First Crystallographically Characterized Complex Containing the $W_2(O)_2(\mu\text{-}O)(\mu\text{-}S)$ Unit

Shinji Ikari, Yoichi Sasaki,* and Tasuku Ito*

Received July 13, 1988

Neutralization by aqueous 2 M Na_2CO_3 of an H_2S-saturated aqueous solution of $(NH_4)_2[WOCl_5]$ and disodium dihydrogen ethylenediaminetetraacetate (Na_2H_2edta) gave a mixture of the title complex and the known $[W_2(O)_2(\mu\text{-}O)_2(\mu\text{-edta})]^{2-}$. The new complex was purified by the use of an anion-exchange column (QAE-Sephadex A-25). The crystal of $Ba[W_2(O)_2(\mu\text{-}O)(\mu\text{-}S)(\mu\text{-edta})]\cdot 6.5H_2O$ ($W_2BaSO_{17.5}N_2C_{10}H_{25}$) is orthorhombic, space group *Fdd*2, with a = 25.323 (1) Å, b = 50.706 (5) Å, c = 7.077 (1) Å, V = 9087.5 (4) Å^3, and Z = 16. The structure was solved by using 4075 unique reflections with $|F_o| > 3\sigma(F_o)$ to give R = 0.034. The metal-to-metal distance is 2.654 (1) Å, which is in the range of a direct metal–metal bond. Bond distances and angles within the $W_2(O)_2(\mu\text{-}O)(\mu\text{-}S)$ moiety are very similar to those of the known $Mo_2(O)_2(\mu\text{-}O)(\mu\text{-}S)$ unit. $[W_2(O)_2(\mu\text{-}O)(\mu\text{-}S)(\mu\text{-edta})]^{2-}$ exhibits absorption peaks at 440 nm (ϵ = 240 M^{-1} cm^{-1}) and 273 (9430) in water. Cyclic voltammetry in aqueous solution (pH 7.5, 0.2 M phosphate buffer) shows one irreversible oxidation wave at +0.65 V vs SCE with a glassy-carbon electrode. ^1H and ^{13}C NMR spectra in D_2O are consistent with the rapid inversion of the pseudo-gauche structure of the N–C–C–N bridge. The XPS spectrum in the solid state indicates binding energies of the metal 4d and 4f electrons lower than those of $[W_2(O)_2(\mu\text{-}O)_2(\mu\text{-edta})]^{2-}$.

Introduction

Molybdenum(V) is known to form preferably dimeric complexes with the $Mo_2(O)_2(\mu\text{-}O)_2$ core in aqueous media. All the bridging and terminal oxide ions can successively be replaced by sulfide ions, and the following cores are now known: $Mo_2(O)_2(\mu\text{-}O)(\mu\text{-}S)$, $Mo_2(O)_2(\mu\text{-}S)_2$, $Mo_2(O)(S)(\mu\text{-}S)_2$, and $Mo_2(S)_2(\mu\text{-}S)_2$.[1] Tung-

0020-1669/89/1328-0447$01.50/0